Purdue University
Purdue e-Pubs

International Compressor Engineering Conference   School of Mechanical Engineering

2016

Integrating Numerical Models for Efficient Simulation of Compressor Valves

Ajay Parihar
Emerson Climate Technologies, ajay.parihar@emerson.com

David Myszka
University of Dayton, United States of America, dmyszka@udayton.edu

Benjamin Robinet
Emerson Climate Technologies, benjamin.robinet@emerson.com

Thomas Hodapp
Emerson Climate Technologies, Thomas.Hodapp@emerson.com

Follow this and additional works at: https://docs.lib.purdue.edu/icec

Integrating Numerical Models for Efficient Simulation of Compressor Valves

Ajay PARIHAR[1], David MYSZKA[2]*, Benjamin ROBINET[1], Thomas HODAPP[1]

[1]Emerson Climate Technologies, Applied Mechanics
Ajay.Parihar@Emerson.com, Benjamin.Robinet@Emerson.com, Thomas.Hodapp@Emerson.com

[2]University of Dayton, Department of Mechanical and Aerospace Engineering
Dayton, OH, USA
dmyszka@udayton.edu

* Corresponding Author

ABSTRACT

The motion of automatic, self-acting valves is a primary aspect in achieving superior compressor reliability and performance. Simulation of compressor valve mechanics involves a complex set of interactions that include characteristics of the compression chamber, thermodynamics, gas flow, valve motion, and pressure pulsations through the valve passages. One-dimensional (1D) lumped simulation models that encompass these interactions have been formulated and refined over the past several decades. During that same time period, finite element theory for fluid-structural-interaction (FSI) has been developed. FSI provides three-dimensional (3D) results across the entire fluid and solid domain and is well-suited for compressor simulation. However, the usage of FSI on real problems has not been adopted until much more recently, as sufficient computational resources became available. Still, the high computational expense and significant run times create a practical barrier to using FSI as a routine design tool.

This paper presents techniques for integrating 1D-lumped models with 3D-FSI models. Methods to properly formulate the 1D-models are discussed. Once formulated, these 1D-models provide quick and accurate results that are used to narrow various design alternatives. Additionally, the 1D-models provide initial conditions for the higher resolution 3D-FSI models in critical regimes of operation. Lastly, experimental data is shown to confirm the techniques.

1. INTRODUCTION

The design of valve systems has a strong influence on the cost, performance and reliability of compressors. The primary function of a valve is to permit gas flow and prevent reverse flow. For compressor efficiency, self-acting valves should have a quick response and not impede the forward flow. The durability of valves is threatened as they are subjected to reversed stress and impacts, repeated with each rotation of the crank shaft.

Numerical valve simulation has long been the focus of research projects. Over thirty years ago, Soedel (1984) compiled a short course that presented simulation strategies for the compression chamber, valve dynamics and gas pulsations through the suction and discharge passages. These models predict aggregate measures of compressor performance including mass flow, capacity, power consumption and efficiency. Additionally, the models predict pressure pulsation levels, valve stresses and impact velocities. These simulations are termed one-dimensional (1-D) lumped models as they assume one-dimensional flow or refrigerant, consider the average properties within the compression chamber and use minimal degrees of freedom to track the motion of the valves.

Several subsequent developments have been made to the original 1-D-lumped models outlined by Soedel. Fagotti et al. (1996) increased the degrees of freedom of reed valve motion model by adopting a finite element approach. Bukac (2002) accounted for the flexibility of the valve lift-limiter (stop) and seat. Khalifa and Liu (1998) derived an expression for adhesion force caused by the interfacial surface tension of the lubricating oil film between the valve and seat, which is often termed a stiction force. Pizarro-Recabarren et al. (2012) expanded on that expression to consider the existence of a finite amount of oil between the valve and the seat.

A second, more recent, option for compressor valve simulation is a finite element analysis scheme that is adapted for systems that involve fluid-structural-interaction (FSI). FSI is encountered when fluid flow causes deformation of a structure, which alters the boundary conditions of the fluid flow. With the development of high performance computing, it has become possible to analyze complex systems with a coupling of fluid and structural dynamics. For a compressor, FSI offers a refined examination of the three-dimensional (3D) variation of mechanical properties across the entire fluid and solid domains.

Several studies using FSI models to simulate compressor behavior are found in the literature. Bassiouny and O'Neal (2004) first demonstrated the use of FSI analysis on refrigerant flow through a short flexible tube. Kim et al. (2008) expanded an FSI to a reciprocating compression chamber with a focus on discharge valve impacts. Wu et al. (2012) showed the importance of including the suction and exhaust systems within the FSI analysis.

While the fidelity of the FSI results are superior, the computational expense prevents it being used as a routine design tool. A pragmatic approach is to use a combination of the FSI and 1-D lumped models to explore compressor design options. Such an approach advocates that the 1-D lumped model be used for broad design studies, while the FSI model is used to make final adjustments. Mayer et al. (2014) conducted a study to compare the results from an FSI model and a basic 1-D lumped model. This paper presents strategies for both the FSI and 1-D lumped models to facilitate convergence between the methods and agreement with experimental results. The remainder of the paper is organized as follows. Section 2 presents the 1-D lumped models used by the authors. Section 3 shows an overview of FSI. Section 4 presents the modeling techniques used in three examples that illustrate correlation between 1-D lumped models, FSI, and experimental results.

2. ONE-DIMENSIONAL LUMPED SIMULATION MODEL

A schematic of a 1D-lumped model for a single cylinder reciprocating compressor is shown in Fig. 1. Since many versions of a 1-D lumped models have been implemented and discussed in the literature, the methods used by the authors is detailed in the following sections. While a reciprocating compressor is illustrated, the modeling approach applies to any compression technologies.
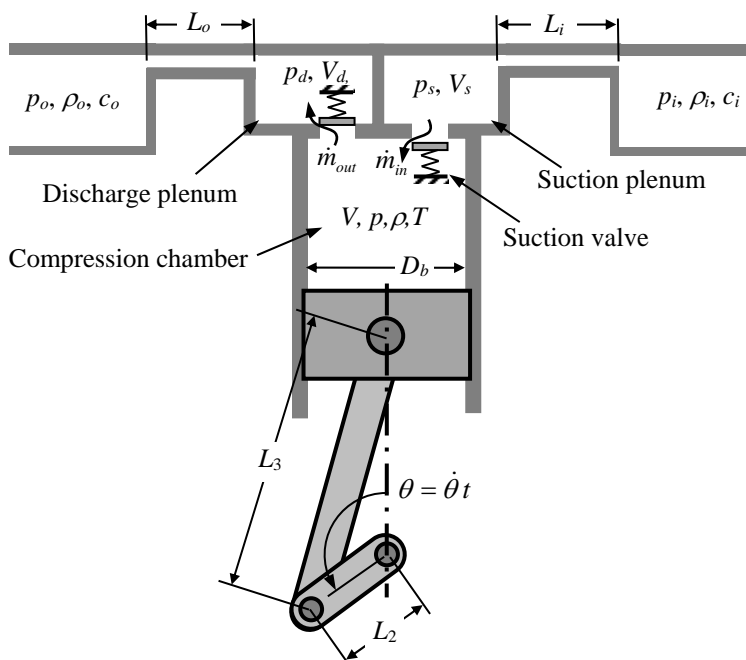

Figure 1: Schematic of a 1D-lumped model for a single cylinder reciprocating compressor.

2.1 Compression Chamber Volume
Closed form equations for the volume of a compression chamber should be generated. For the case of a reciprocating compressor, the volume at a crank angle θ with a bore diameter D_b, crank length L_2, connecting rod length L_3, and clearance volume V_c is

$$V = V_c + \frac{\pi D_b^{\,2}}{4}\left[L_2(1-\cos\theta) + L_3\left(1 - \sqrt{1 - \left(\frac{L_2}{L_3}\sin\theta\right)^2}\right)\right] \tag{1}$$

The time derivative of Eq. (1) is a necessary value and is

$$\frac{dV}{dt} = \frac{dV}{d\theta}\frac{d\theta}{dt} = \frac{\pi\,\dot\theta\,D_b^{\,2}L_2}{4}\left(\sin\theta + \frac{L_2\sin\theta\cos\theta}{\sqrt{L_3^{\,2} - L_2^{\,2}\sin^2\theta}}\right) \tag{2}$$

where $\dot\theta$ is the speed of the crank shaft.

2.2 Compression Chamber Density

Conservation of mass within the compression chamber is used to derive an expression for the density ρ. Considering the change of mass $dm/dt = d(\rho V)/dt$, and expanding gives

$$\frac{d\rho}{dt} = \frac{1}{V}\left[\dot{m}_{in} - \dot{m}_{out} - \rho\frac{dV}{dt}\right] \tag{3}$$

2.3 Compression Chamber Pressure and Temperature

Energy balance models are commonly used to generate expressions for the temperature T within the compression chamber (Chen et al., 2002). However, obtaining reliable heat transfer coefficients through the cylinder walls can prove to be problematic. Alternatively, the polytropic compression model, $p/\rho^\gamma = \text{constant}$, can be used to develop an expression for the pressure p within the compression chamber,

$$\frac{dp}{dt} = \frac{p\gamma}{\rho}\frac{d\rho}{dt} \tag{4}$$

where γ is a polytropic exponent that can be judiciously predicted (Lenz, 2002). The corresponding temperature within the compression chamber can be determined from the density and the pressure by implementing equations of state, with queries to a refrigerant property database, such as REFPROP (Lemmon et al., 2010), or lookup tables (Laughman et al., 2012).

2.4 Flow through Suction and Discharge Ports

A one-dimensional, isentropic flow model is commonly applied to generate expressions for the flow through the ports. The mass flow through the suction port is

$$\dot{m} = \rho_u (CA)\, c \sqrt{\frac{2}{\kappa - 1}\left[\left(\frac{p_u}{p_d}\right)^{1-\kappa/\kappa} - 1\right]} \tag{5}$$

where p_u is the upstream pressure, p_d is the downstream pressure, C is the flow coefficient, A is the effective flow area, c is the speed of sound in the refrigerant, and κ is the ratio of specific heats (c_v/c_p). Schwerzler and Hamilton (1972) developed a widely-adopted method for determining appropriate flow area CA values for the ports as a function of valve displacement. Equation (5) is applied to both the suction and discharge valves.

2.5 Valve Motion

Some compressors use translating poppet valves that can be accurately modeled as a single degree of freedom. The displacement w is governed by

$$M\,\ddot{w} + C_1\,\dot{w} + C_2\,|\dot{w}|\,\dot{w} + K\,w = F(t) \tag{6}$$

where K is the stiffness of a valve spring, M is the equivalent valve mass (which includes a portion of the valve spring), $\dot{w}$ is the valve velocity, and $\ddot{w}$ is the valve acceleration. Damping is partitioned into a linear term to simulate structural or viscous damping and a second-order term to simulate high-velocity flow damping. Both terms are represented by coefficients C_1 is C_2, respectively. As with CA, Schwerzler and Hamilton (1972) developed an expression for the force on a valve as

$$F(t) = FA\big(p_u - p_d\big) \tag{7}$$

and outlined a process for determining effective force area *FA* values for the ports as a function of *w*. Equation (6) is applied to both the suction valve (with displacement w_s) and discharge valve (with w_d).

Translating disc style valves have a single degree-of-freedom (dof) and naturally behave according to Eq. (6). Flexible valves can be modeled as an equivalent single dof system, or with a finite element approach as discussed below. Expressing the valve velocity as $\dot{w}$, constraints must be applied to enforce that the valve does not penetrate the valve seat or stop, if one is used. Thus, $0 < w < w_{max}$, where w_{max} is the maximum valve displacement permitted by a valve stop. Additionally, it is common to assume that the valve bounces off the seat or backer with a coefficient of restitution C_R. Thus, if $w = w_{max}$ or $w = 0$, then $\dot{w} = -C_R \dot{w}$. The conditions are enforced for the suction and discharge valves.

A finite element approach can be used to more accurately model the distributed mass and elasticity of the flexible valves. This approach is particularly useful when the boundary conditions of the attachments and backer are difficult to approximate with a single degree of freedom. In this case, the coefficients of Eq. (6) become matrices. A two-node plane Bernoulli-Euler beam element that has length ℓ_v^e, thickness t_v, average element width b_v^e and uniform mass density ρ_v has element mass and stiffness matrices as

$$M^e = \frac{\rho_v t_v b_v^e \ell_v^e}{420} \begin{bmatrix} 156 & 22\ell & 54 & -13\ell \\ 22\ell & 4\ell^2 & 13\ell & -3\ell^2 \\ 54 & 13\ell & 156 & -22\ell \\ -13\ell & -3\ell^2 & -22\ell & 4\ell^2 \end{bmatrix} \quad K^e = \frac{E_v b_v^e (t_v)^3}{12(\ell_v^e)^3} \begin{bmatrix} 12 & 6\ell & -12 & 6\ell \\ 6\ell & 4\ell^2 & -6\ell & 2\ell^2 \\ -12 & 13\ell & 12 & -6\ell \\ 6\ell & 2\ell^2 & -6\ell & 4\ell^2 \end{bmatrix} \tag{8}$$

The element matrices in Eq. (8) are assembled into a global set of equations and reduced according to boundary conditions.

2.6 Plenum Pulsations
With a finite volume of the suction and discharge plenum and intermittent flow through the ports, a time-varying pressure pulse is created behind the valves. A common model for the passages consists of a cavity connected by a relatively short tube into a larger collecting tank with steady conditions. The Helmhotz principle can be used to model the motion of a slug of gas within the tube (Soedel, 1973). Considering the discharge passage with discharge volume V_d, a tube length L_o, area A_o terminating with steady pressure, density and speed of sound conditions of p_o, c_o, ρ_o, the resonator equation is

$$L_o A_o \rho_o \ddot{\xi} + D_o \dot{\xi} + \frac{c_o^2 \rho_o A_o^2}{V_d} \xi = \frac{c_o^2 A_o}{V_d} \int_0^t \dot{m}_{out} \, dt \tag{9}$$

where ξ is the movement of gas through the tube. Equation (9) is also written for the suction passage and can be solved having the mass flow rate through the valves in Eq. (5). The time-varying pressure behind the valve is obtained once the movement of gas through the passage ξ is known.

$$p_d = \frac{c_o^2}{V_d} \int_0^t \dot{m}_{out} - \frac{c_o^2 \rho_o A_o}{V_d} \xi + p_o \tag{10}$$

2.7 Valve Stiction
Adhesion (or stiction) is a source of thermodynamic and volumetric losses in the compressor as a higher pressure difference is required to open the valve, which subsequently delays in the valve opening. Stiction is attributed to the presence of a lubricant oil film between the valve and the seat. The stiction force results from a combination of interfacial tension, capillarity effects and deformation (viscous flow) of the oil film. An expression (Khalifa and Liu, 1998) depends on the valve lift, valve velocity, lubricant viscosity μ, effective inner and outer contact radii of the valve and seat, r_i and r_o.

$$F_{st} = \mu (r_o - r_i)^3 (r_o + r_i) \frac{\dot{w}}{w^3} \tag{11}$$

The stiction force of Eq. (11) will appear as an additional term on the right side of Eq. (7).

2.8 Solution

Equations (3), (4), (7) and (9) are time-based, ordinary differential equations (ODEs) of the form $dx(t)/dt = f(x(t))$, where $x(t) = [\rho, p, w_s, \dot{w}_s, w_d, \dot{w}_d, \xi_s, \dot{\xi}_s, \xi_d, \dot{\xi}_d,]$. Explicit numerical methods are commonly used to solve ODEs of this form. To start the solution process, a set of initial conditions $x(0)$ must be specified. For reciprocating compressor simulation, TDC is commonly used. The Runge-Kutta technique is a commonly used explicit method to progressively step through a time interval by determining a new set of simulation values $x(t_{n+1})$ using the set of values already known $x(t_n)$. The routine iterates through multiple crank rotations, checking whether the conditions at 0° are equal to those at 360°, $x(t_{0°}) = x(t_{360°})$. Additionally, the total mass flow leaving the compressor must equal to the total mass flow entering the compressor.

3. THREE DIMENSIONAL, FLUID-STRUCTURAL INTERACTION MODELS

In FSI analysis, fluid forces are applied onto the solid and the solid deformation changes the fluid domain. The computational domain is typically divided into separate discretized fluid and solid domains. The fluid and solid models are defined respectively, through their material data, boundary conditions, etc. Fig. 2 shows a flow chart of the solution process.
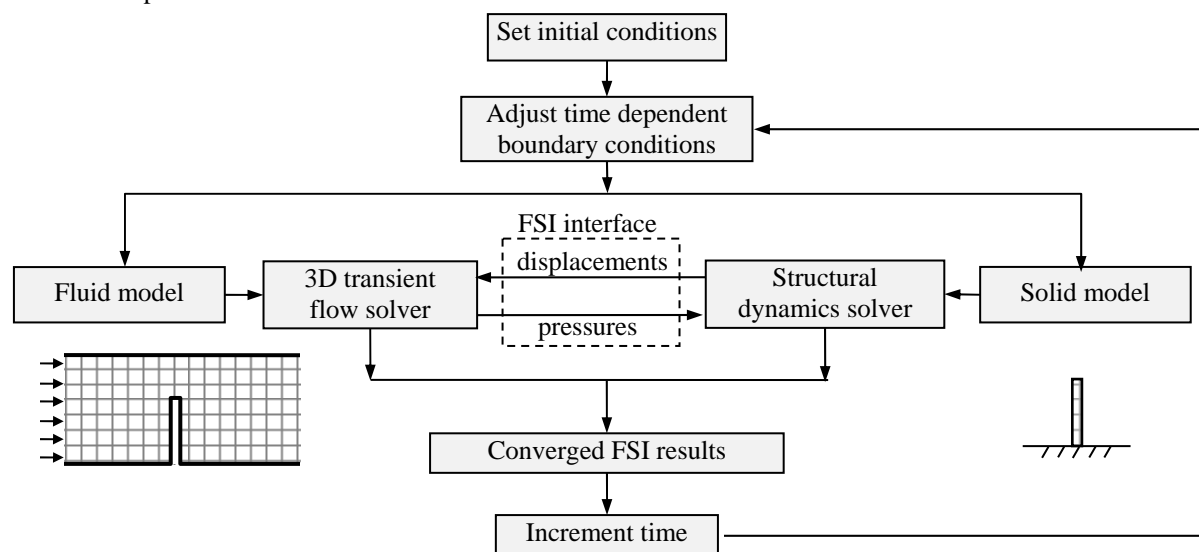

Figure 2: FSI simulation flow chart.

3.1 Transient Fluid Dynamics

The computational fluid dynamics (CFD) model is defined with a spatial fluid domain, wall boundary conditions, and the fluid-structure interface condition. In addition to the interface condition, the fluid domain may have prescribed changes with time (ie., a moving mesh).

Fluid solver involves the Navier-Stokes equations, which are expressed as a continuity equation, three directional momentum equations and an energy equation. In order to obtain a closed system for solution variables, additional equations, such as equations of state and turbulence models for the fluid under consideration must be provided.

3.2 Structural Dynamics

The structural finite element analysis (FEA) model involves the valve components, including the reed, attachment hardware, and backer. The structural dynamics solver involves a traditional, transient dynamic finite element method similar to that shown in Eq. (8).

3.3 Solution Parameters

Most commercial packages use an iterative coupling approach as shown in Fig. 2, where the equations governing the flow and the displacement of the structure are solved separately with two distinct solvers. Apart from standard boundary conditions applied, an FSI boundary is declared at the interface of fluid and solid models to transfer the

loads in two-way coupled fashion. FSI simulation requires smaller time step size to resolve the flow gradients and contact convergence on solid side for valve applications. Sufficient number of iterations is given to converge the solution per time step as well as to converge load transfer across two solvers. Higher order discretization schemes in space and time is used for better accuracy of results.

4. TECHNIQUES DEVELOPED FOR USING THE MODELS

Strategies for using the 1-D lumped model and FSI model to facilitate convergence between the methods and agreement with experimental results is presented.

4.1 Techniques for using the 1D-Lumped Model

As an application example, a three-cylinder compressor shown in Fig. 3 contains a flexible suction valve and translating discharge valve. When the objective of the simulation is to determine the performance implications of valve size and arrangements, an equivalent single-dof valve model is deemed sufficient.
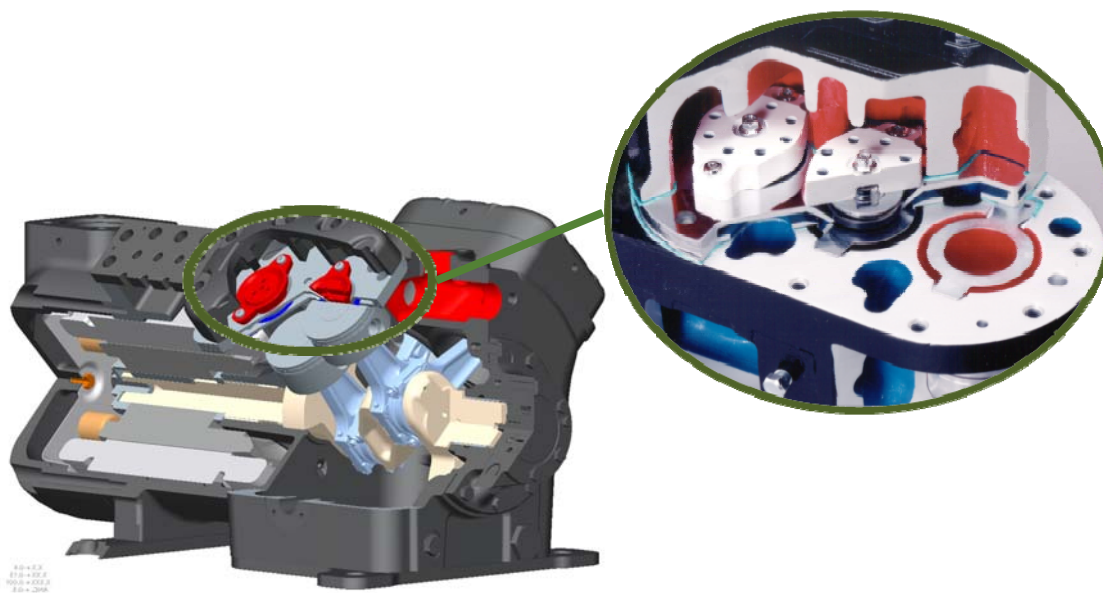

Figure 3: Reciprocating compressor with a flexible discharge valve and translating (Discus) discharge valve.

For flexible reed valves, the centroid of the port is used as the reference point for displacement coordinate. Thus, all distributed properties are lumped to that point on the valve.

The equivalent valve stiffness can be determined through classical beam theory, finite element analysis, or experimentally if physical parts are available. Experimental determination of stiffness is preferred when stacked valve components are used, as there is uncertainty in the friction values between the stacks. The equivalent valve mass can be determined through energy-equivalency methods or FEA modal analysis.

Contact with valve stops alter the boundary conditions for the valve dynamics. The equivalent single-dof lumped valve stiffness and lumped mass is determined within the bounds of the various boundary conditions. A lookup table is generated to provide appropriate values at increments of valve lift, to distinguish changes in the constraints.

The effective flow area *CA* and effective force area *FA* approach is incorporated. Instead of using an experimental setup described by Schwerzler and Hamilton (1972), CFD models are used to determine the flow area *CA* and the force area *FA* at various valve displacements. A steady-state analysis is performed on a fluid domain constructed upstream, downstream and through the port, with the valve set at a prescribed displacement. An arbitrary mass flow

and downstream pressure is specified. Using the CFD results, the upstream pressure and force exerted onto the valve model is tabulated. Values for *CA* and *FA* at that prescribed displacement are determined from Eqs. (5) and (7).

Using the approach above, aggregate measures of compressor performance, namely mass flow and power, have typically been within 3%. Figure 4 illustrates comparison of the 1-D model with a compressor that was instrumented with a pressure transducer. It is noted that for compressors with low volumetric clearance, the volume under the valve as it displaces is included in the compression chamber, which improve correlation.
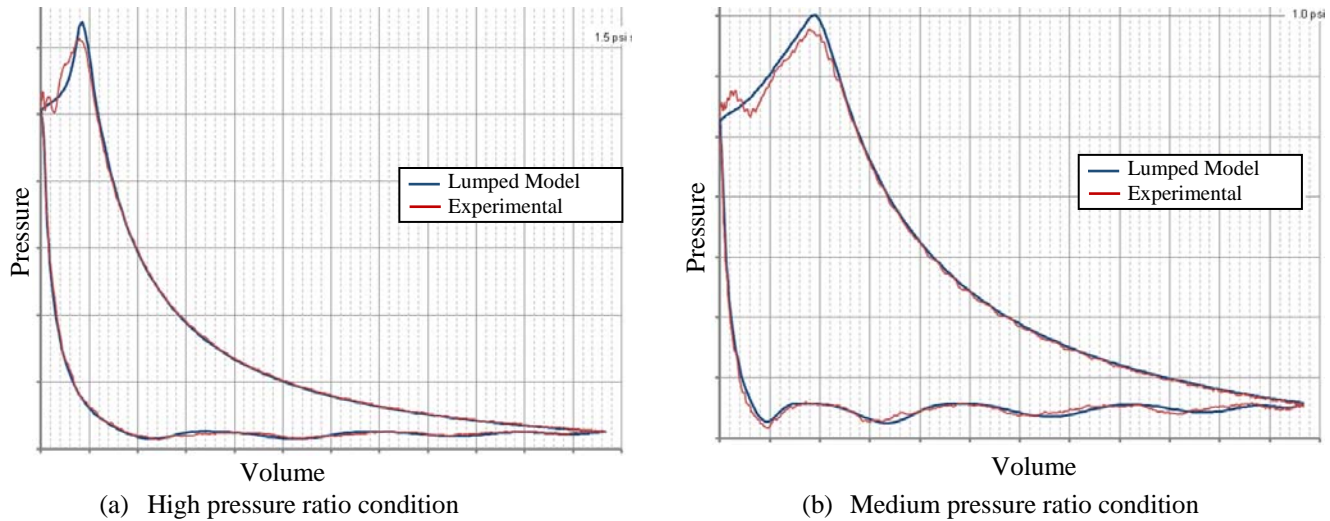

(a) High pressure ratio condition	(b) Medium pressure ratio condition

Figure 4: 1-D lumped model comparisons with experimental pressure-volume data.

To more accurately determine stress and impact velocities of flexible valves, a finite element approach of Eq. (8) replaced the single dof valve model. For Eq. (7), the forcing function was distributed across the area projected by the port. Comparison of a multiple dof valve within the lumped model is provided in the following section.

4.2 Techniques for using the FSI Model

A second application example is shown in Fig 5, containing a four-cylinder compressor with two flexible suction and two flexible discharge valves in each cylinder. The focus of the study is to predict dynamic stresses and impact of the suction valve by performing three-dimensional transient FSI simulation
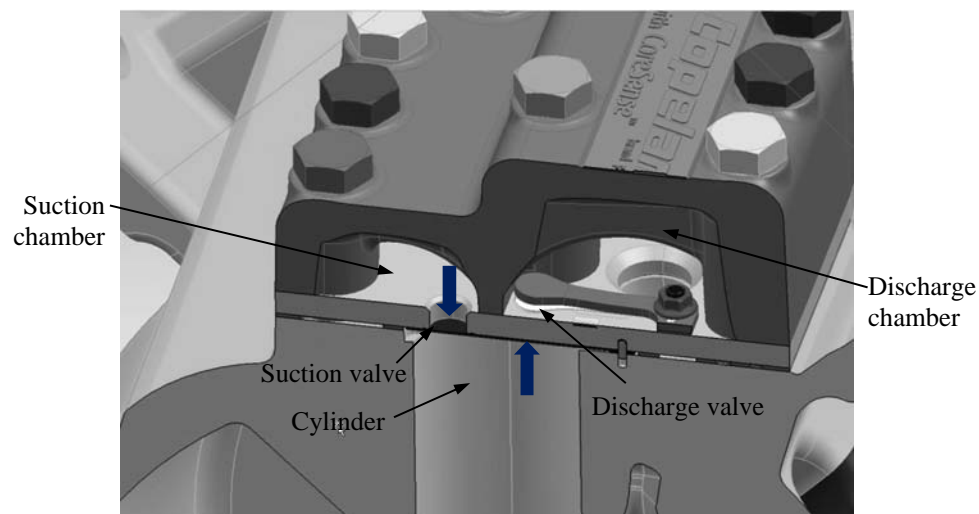

Figure 5: Refrigeration compressor arrangement of cylinder, suction and discharge valves and passages.

Due to symmetry, half a cylinder was modeled. A fluid domain included the inlet plenum chamber, valve passge, and compression chamber as shown in Fig. 6a. The compression chamber had a time-varying moving mesh that was synchronized with movement of the top of the cylinder. With a symmetry model, a single suction reed valve was model, as shown in Fig. 6b. Boundary conditions included a fixed end and valve stop. As is typical for a compressor FSI model, the fluid domain included nearly 50 times more elements as the solid mesh. The surfaces exposed to the fluid were defined as the FSI interface. Zero shear was specified at the symmetry face. All other faces were defined as no-slip boundary condition.
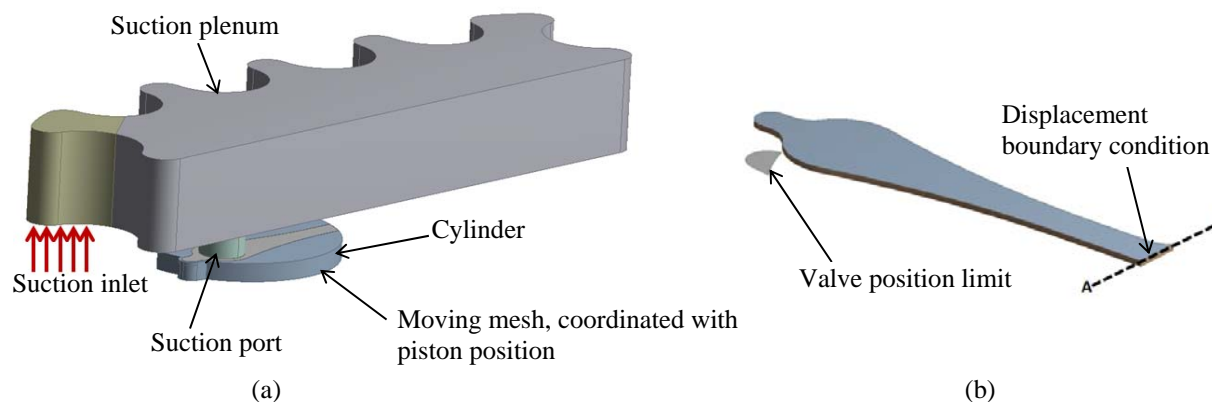

Figure 6: Fluid (a) and structural (b) models for compressor FSI analysis

Suction pressure and temperature were specifed as inlet boundary condition as shown in Fig 6a. The top dead center position of the piston served as the initial condition. The suction pressure and temperature were used with REFPROP to provide initial refrigerant properties. Flow was modeled as turbulent using standard k-epsilon model along with Redlich-Kwong, real gas density formulation (Redlich, Kwong, 1949). The SIMPLE scheme (Patankar et. al., 1972) is used for pressure-velocity coupling, whereas mesh displacement is solved using a direct sparse solver (Angeleri et al., 1989) on the structural side. To speed up the overall simulation time, a variable time step size is used by keeping smaller time step size at the time of valve opening and closing to resolve the steep flow gradients.

A lumped model of the compressor was also constructed using the techniques described in the previous section. A finite element approach (ie., Eq. (8)) was used to model the valve, using 10 nodes. The displacement of each node was limited to motion between valve plate and stop. Figure 7 illustrates comparison of valve displacement and velocity from the FSI model and the lumped model.
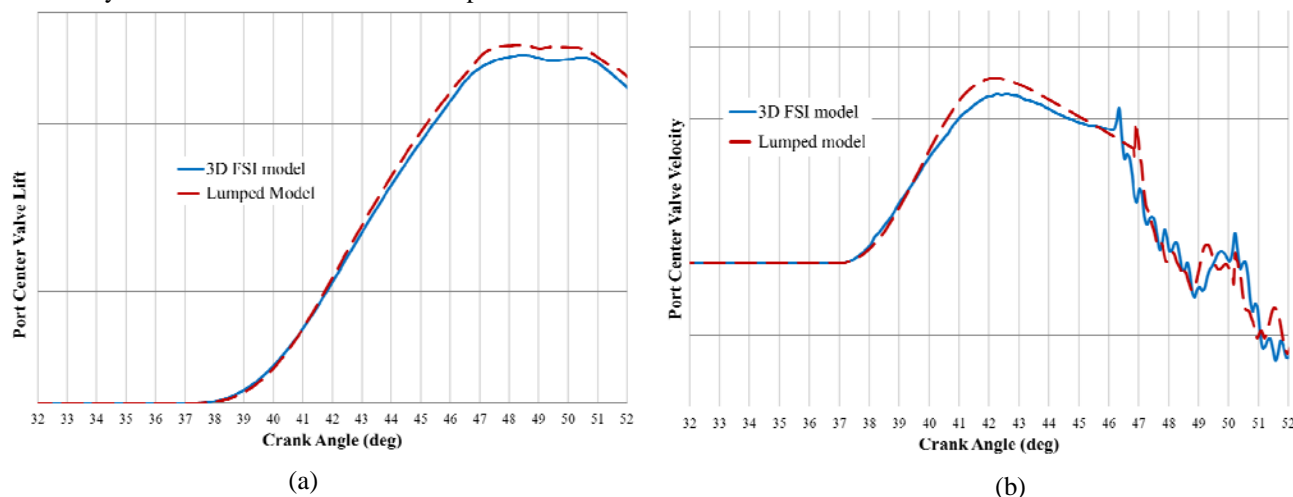

Figure 7: Comparison of (a) displacement and (b) velocity results for lumped and FSI models.

The FSI methodology described above was used to study the flexible discharge reed dynamics. FSI result comparisons were made with a compressor equipped with strain gages on the discharge reed. Three gages were placed (1) at the port center, (2) at mid-length on the edge of the reed, and (3) at the clamped end on the edge of the reed. The comparison of the FSI and strain gage results are shown in Fig 8. The FSI model results were within 3%, 5%, and 7%, respectively.
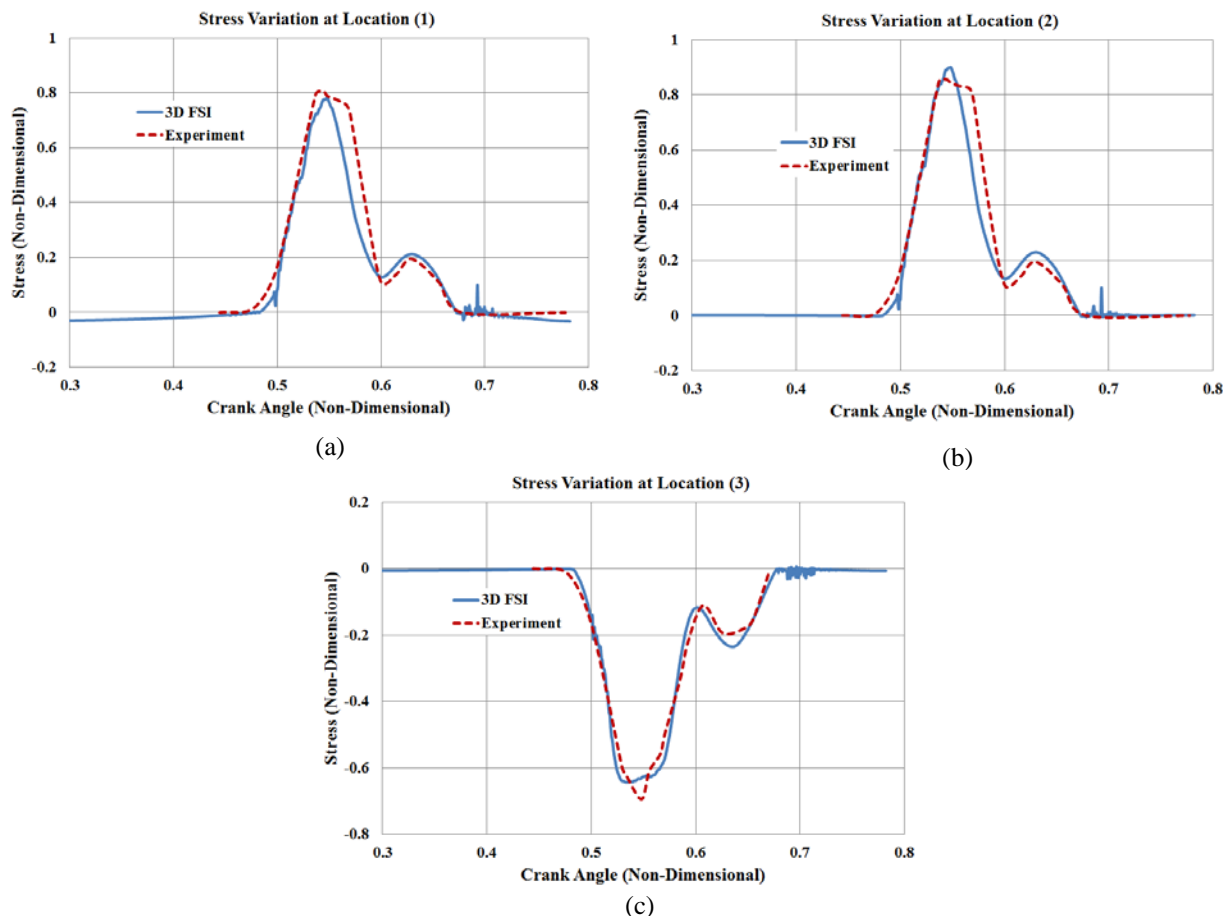

(a)

(b)

(c)

Figure 8: Comparison of FSI valve strain results with experimental strain gage values

5. CONCLUSIONS

This paper presented techniques for compression, flow and valve simulations using both 1D-lumped and 3D-FSI models. Detailed equations and methods to effectively formulate the lumped models are provided. Approaches for using commercial FSI software are discussed. Correlations between the lumped model, 3D-FSI model, and experimental data are shown to confirm the techniques.

This paper illustrates that both models can be used in complimentary fashion within a commercial product development environment. The FSI models provide a superior fidelity, but come at a computational cost. At this time, it is unreasonable to complete a full cycle FSI analysis on numerous design alternatives. Properly formulated, lumped models provide quick and accurate results that can be used to narrow various design alternatives. Additionally, the lumped models can be used to provide initial conditions for the higher resolution 3D-FSI models to be solved in critical regimes of operation.

REFERENCES

Angeleri, F., Sonnad, V., Bathe, K-J. (1989) Studies of finite element proceduresan evaluation of preconditioned iterative solvers, *Computers and Structures*, Vol 32, No. 3-4, pp. 671-677.

Bukac, H. (2002) Understanding Valve Dynamics, *Proc. of the Int. Compressor Eng. Conf. at Purdue*, Paper No. 1564.

Baassiouny R., O'Neal, D. (2004) Analysis Of Refrigerant Flow and Deformation for a Flexible Short-Tube using a Finite Element Model, *International Journal of Refrigeration*, Vol. 27, No. 1, pp. 176-183.

Chen, Y., Halm, N.P., Groll, E.A., Braun, J.E. (2002) Mathematical modeling of scroll compressors - part i: compression process modeling, , *International Journal of Refrigeration,* Vol. 25, No. 6, pp. 731-750.

Fagotti, F., de Bortoli, M., Barbieri, R. (1996) A Finite Element Approach to Compressor Valves Motion Simulation, *Proc. of the Int. Compressor Eng. Conf. at Purdue*, Paper No. 1132.

Khalifa, H., Liu, X. (1998) Analysis of Stiction Effect on the Dynamics of Compressor Suction Valve, *Proc. of the Int. Compressor Eng. Conf. at Purdue*, Paper No. 1221.

Laughman, C., Zhao, Y., Nikovski, D. (2012) Fast Refrigerant Property Calculations Using Interpolation-Based Methods, *Proc. of the Int. Compressor Eng. Conf. at Purdue*, Paper No. 1344.

Lenz, J. (2002) Polytropic Exponents for Common Refrigerants, *Proc. of the Int. Compressor Eng. Conf. at Purdue*, Paper No. C9-3.

Lemmon, E.W., Huber, M.L., McLinden, M.O. (2010) *NIST Standard Reference Database 23: Reference Fluid Thermodynamic and Transport Properties-REFPROP*, Version 9.0, National Institute of Standards and Technology.

Mayer, J., Bjerre, P., Brune, F. (2014) A Comparative Study Of Different Numerical Models For Flapper Valve Motion, *Proc. of the Int. Compressor Eng. Conf. at Purdue*, Paper No. 2309.

Patankar, S., Spalding, D. (1972), "A calculation procedure for heat, mass and momentum transfer in three-dimensional parabolic flows", *Int. J. of Heat and Mass Transfer*, Vol. 15, No. 10, pp. 1787-1806.

Pizarro-Recabarren, R., Barbosa, J., Deschamps, C. (2012) Modeling the Stiction Effect in Automatic Compressor Valves, *Proc. of the Int. Compressor Eng. Conf. at Purdue*, Paper No. 2044.

Redlich, O., Kwong, J. (1949). On Thermodynamics of Solutions, *Chemical Reviews,* Vol. 44, No. 1, pp. 233–244.

Soedel, W. (1984) *Mechanics, Simulation and Design of Compressor Valves, Gas Passages and Pulsation Mufflers,* Ray W. Herrick Laboratories, School of Mechanical Engineering, Purdue University.

Soedel, W. (1984) On Helmholtz resonator effects in the discharge system of a two-cylinder compressor, *MJ. of Sound and Vibration,* Vol. 30, No. 3, pp. 263-277.

Schwerzler, D., Hamilton, J. (1972) An Analytical Method for Determining Effective Flow and Force Areas for Refrigeration Compressor Valving Systems (1972). *Proc. of the Int. Compressor Eng. Conf. at Purdue*, Paper No. 5.

Kim, H., Ahn, J., Kim, D. (2008) Fluid Structure Interaction and Impact Analyses of Reciprocating Compressor Discharge Valve, *Proc. of the Int. Compressor Eng. Conf. at Purdue*, Paper No. 1936.

Wu, S., Wang, Z. (2014) A Numerical Simulation of Fluid-Structure Interaction for Refrigerator Compressors Suction and Exhaust System Performance Analysis, *Proc. of the Int. Compressor Eng. Conf. at Purdue*, Paper No. 1131.

ACKNOWLEDGEMENT